Soft Matter

Effect of Equilibration Time on the Structural Gradient in the Vertical Direction for Bicontinuous Microemulsions in Winsor-III and -IV Systems

Journal:	*Soft Matter*
Manuscript ID	SM-ART-12-2023-001741.R1
Article Type:	Paper
Date Submitted by the Author:	01-Apr-2024
Complete List of Authors:	Hayes, Douglas; University of Tennessee Knoxville, Biosystems Engineering and Soil Science Barth, Brian; University of Tennessee Knoxville, Chemical and Biomolecular Engineering Pingali, Sai Venkatesh; Oak Ridge National Laboratory, Biology and Soft Matter Division

Effect of Equilibration Time on the Structural Gradient in the Vertical Direction for Bicontinuous Microemulsions in Winsor-III and -IV Systems

Douglas G. Hayes*[,1], Brian A. Barth[2], Sai Venkatesh Pingali*[,3]

[1] Department of Biosystems Engineering and Soil Science, University of Tennessee, 2506 E.J. Chapman Drive, Knoxville, TN 37996-4531, dhayes1@utk.edu , 1-865-974-7991, ORCID 0000-0003-0303-1411

[2] Department of Chemical and Biomolecular Engineering, University of Tennessee, 1512 Middle Dr, Knoxville, TN 37996, bbarth@vols.utk.edu ORCID: 0000-0002-3887-6054

[3] Oak Ridge National Laboratory, 1 Bethel Valley Road, Oak Ridge, TN 37831, pingalis@ornl.gov ORCID: 0000-0001-7961-4176

1 April 2024

ABSTRACT

Bicontinuous microemulsions (BMEs), self-assembly systems consisting of oil and water nanodomains separated by surfactant monolayers, have many applications. However, changes in structure and properties of BMEs in the vertical direction can affect BMEs' utility. This study's objective was to determine the effect of equilibration time (τ_{eq}) on structural changes in the vertical direction for bicontinuous phases of Winsor-III (W_{III}) systems *in situ* or after being isolated, for D_2O+H_2O/1-dodecane/sodium dodecyl sulfate (SDS)/1-pentanol/NaCl at 22°C. Small-angle neutron scattering (SANS) measurements were performed using a vertical stage sample environment that precisely aligned samples in the neutron beam. SANS data were fitted by the Teubner-Strey (TS) model and changes in TS-derived parameter values were observed. For 10 min $\leq \tau_{eq} \leq$ 4 h, the effective activity of the bicontinuous phase's surfactant monolayers increased with time at all vertical positions. At short equilibration (τ_{eq} =10 min), small but significant amounts of water and oil were transiently emulsified near the W_{III} upper liquid-liquid interface. W_{III} systems underwent a relaxation process after being transferred to narrow 1 mm pathlength cells, resulting in a decrease of surfactant activity for the top half of the bicontinuous phase. For isolated bicontinuous phases, results suggest that SDS was desorbed from the BMEs by quartz near the bottom, while near the top, the water concentration near was relatively high. The results suggest that W_{III} systems should equilibrate for at least 4 hours after being prepared and transferred to a container that differs in cross sectional area and surfactant behavior in BMEs can change near interfaces.

KEYWORDS

Bicontinuous microemulsions, small-angle neutron scattering, Teubner-Strey model,Winsor-III microemulsion systems

INTRODUCTION

Bicontinuous microemulsions (BMEs), consisting of thermodynamically stable nanodomains of water and oil separated by surfactant monolayers, are a unique medium potentially useful for many applications, such as enhanced oil recovery (EOR)[1-3], hosting enzyme reactions involving apolar substrates [4], electrolytes for flow batteries [5-7], templating media for nanomaterials[8-12], and drug delivery vehicles [13-15]. BMEs composed of two immiscible polymers and AB-type block copolymers, the latter serving as surfactant, are employed as solid electrolytes for batteries and other materials [16, 17].

Recent studies have focused upon heterogeneity in structure for bicontinuous phase within Winsor-III (W_{III}) systems in the vertical direction. The latter refers to three-phase systems consisting of a middle, bicontinuous phase in equilibrium with water and oil excess phases. The lower, water-bicontinuous phase liquid-liquid interface, possesses ultralow interfacial tension [18]. W_{III} systems have been employed in EOR [1-3] and separations [19, 20]. The systems correspond to the "head" region of the well-known "fish" phase diagrams, referring to the fish-shaped phase boundaries for plots of surfactant concentration vs. tuning parameter (frequently temperature for alkyl ethoxylates and salinity for ionic surfactants) at a fixed water-oil ratio (typically near 1 w/w or v/v) [21]. The head of the fish appears at low surfactant concentrations near an optimal value of the tuning parameter, at which the surfactants are balanced in their hydrophilicity and lipophilicity. One study that focused on the formation process of W_{III} systems detected the

presence of a transient liquid crystalline phase between water and oil phases that disappeared with time as a bicontinuous phase began to form [2]. The authors of the cited study detected a structural gradient in the vertical direction for the bicontinuous phase through small-angle x-ray scattering measurements: an increase of ordering for the bicontinuous phase's surfactant monolayers in the downward direction. Two NMR-based studies found that water concentration increased and oil concentration decreased across the BME W_{III} phase in the downward direction [3, 22]. Previously, we investigated changes of structure of the bicontinuous phase of two W_{III} systems via small-angle neutron scattering (SANS) at 1 mm vertical intervals through use of a vertical stage sample environment, which allowed for precise alignment of the bicontinuous phase in the vertical direction [23]. Through the analysis of SANS data, we found that the degree of ordering changed in the vertical direction but differently between W_{III} systems and that the water concentration increased (oil concentration decreased) slightly in the downward vertical direction. In the cited study, we observed that the changes of structure in the vertical direction appeared to differ with equilibration time.

The objective of the current study is to explore more deeply the impact of equilibration time on the changes of structure in the vertical direction for a W_{III} system formed by water/1-dodecane/sodium dodecyl sulfate (SDS)/1-pentanol/NaCl system near optimal salinity at 22°C [19], one of the two systems we studied previously [23]. During the current study, we observed that changes in structure for the vertical direction were also partially attributable to a relaxation process resulting from the transfer of the W_{III} system to a quartz rectangular cell of small pathlength, attributable to the 4.4-fold decrease of cross-sectional area during the transfer.

One-phase bicontinuous (W_{IV}) systems, when in contact with polar surfaces such as glass, silicon, and clay, undergo ordering near the solid-BME interface (on a sub-microscale),

approaching lamellar structure, especially in the presence of shear, due to the dampening of fluctuations [24-28]. Less efficient surfactants produce bicontinuous phases with gyroid structure near the solid surface [27]. A second objective for the current study is to observe whether similar changes occurred for the bicontinuous phase isolated from the SDS/pentanol W_{III} system and placed in a quartz cell, near the bottom, quartz-BME interface. Such heterogeneity in structure in the vertical direction can affect the properties of nanomaterials formed using BME templates and the diffusive mass transfer rate across interfaces and within the BME phase, which can affect the performance of W_{III} systems for separations and other applications; for example, the performance and properties of nanomaterials formed using bicontinuous templates can be affected. A deeper understanding of the impact of equilibration time and relaxation on bicontinuous phase structure is particularly relevant for separations, since diffusion of solutes across phases occurs shortly after formation of the W_{III} system, likely before the W_{III} system reaches equilibrium [29].

EXPERIMENTAL

Materials

SDS (> 99% pure; specific gravity [SG] = 1.01) was obtained from Avantor Performance Materials (Center Valley, PA, USA). The HPLC-grade solvents 1-dodecane, 1-pentanol, and deuterium oxide (D_2O), SG = 0.749, 0.811, and 1.11, respectively, were obtained from Fisher (Pittsburgh, PA, USA). Deionized water (SG = 0.998), 18 MΩ x cm of resistivity, was used throughout.

Methods

Preparation of W_{III} systems. The SDS/pentanol /dodecane systems were formed according to conditions given in our previous publication [20, 23]. Formation occurred near the optimal salinity (i.e., where surfactants are equally balanced in their hydrophilicity and lipophilicity) at room temperature (22±1°C), leading to a rapid separation of the three phases (typically 1-2 min), with volume fractions of the top, middle (BME) and bottom phases at equilibrium being 0.40, 0.32, and 0.28, respectively [30]. The W_{III} system is characterized in terms of α (mass of oil / mass of water plus oil) of 0.48 and γ (mass fraction of surfactant, i.e., SDS) of 0.021. Phase diagrams for this system have been published elsewhere [31].

W_{III} systems (605 μL) were formed by adding the following solutions to a 2 mL polypropylene microcentrifuge tube (5.1 mm inner diameter) in the following order: 110 μL of 10.0 wt% (0.350 M) SDS in H_2O; 165 μL of 4.00% (0.684 M) NaCl in H_2O/D_2O 1:1 v/v, 275 μL of dodecane, and 55 μL of pentanol. The W_{III} system's oil phase therefore consisted of pentanol/dodecane at 1:5 w/w and the aqueous phase (D_2O/H_2O 30:70 v/v) of 2.4 wt% (0.41 M) NaCl and 3.9% (0.14 M) SDS. The water/oil ratio was 1.2/1.0 w/w. The bicontinuous (middle) phase therefore possessed a bulk neutron contrast between water and surfactant plus oil, with water being 30 vol % deuterated rather than 100% deuterated to reduce the impact of coherent multiple scattering, which adds complexity to the Teubner-Strey (TS) model fitting of SANS data [32, 33]. W_{III} systems were allowed to equilibrate in the microcentrifuge tubes for a specific equilibration time, τ_{eq} (10 min, 1 h, 4 h, 1 d, or 1 mo) prior to SANS analysis. All W_{III} systems employed the same aqueous SDS and NaCl stock solutions and were prepared using the same approach. Shortly before SANS analysis W_{III} samples were carefully transported to custom-made rectangular quartz cells (40 mm height x 15 mm width x 1 mm pathlength) prepared by Hellma Analytics (Müllheim, Germany), thereby exposing the W_{III} system to a 4.4-fold reduction in

cross sectional area. The samples were allowed to equilibrate in the quartz cell until the turbidity disappeared, requiring < 5 min. At this point, the cells were placed in the beam and data collection began. For the sample examining the BME structure for an isolated BME phase, a larger volume of W_{III} sample was prepared and equilibrated for 1 mo; then, the bicontinuous phase was carefully withdrawn and placed in the rectangular quartz cells described above, slightly before measurement by SANS. The isolated bicontinuous phase from the SDS/pentanol W_{III} system remained intact as a single phase for at least several months after being isolated [34].

SANS Analysis. SANS experiments were conducted using the Bio-SANS instrument [35] at Oak Ridge National Laboratory (ORNL), Oak Ridge, TN USA, at room temperature (22±1°C) using the same sample environment and instrument settings as employed previously by us [23]. To achieve an appropriate range of the scattering vector, Q ($4\pi\lambda^{-1}\sin\theta$, where 2θ is the scattering angle and λ the neutron wavelength, 6 Å), 0.003 $Å^{-1} < Q < 0.35$ $Å^{-1}$, two instrument configurations were employed: sample-to-detector distances of 2.5 m (5 guides) and 15.3 m (2 guides), and circular aperture diameters of 40 mm and 2 mm for source and sample, respectively, were implemented. The relative wavelength spread was set to 0.132. The scattering intensity profiles, *I(Q) vs. Q*, were obtained by azimuthally averaging the processed two-dimensional images, which were normalized to incident beam monitor counts, and corrected for detector dark current, pixel sensitivity and background.

The sample environment consisted of a precision vertical stage on which the rectangular cell was mounted [23]. The stage, which can travel a total distance of 40 mm, allowed for vertical scans to be performed at 0.5 mm step size increments. A given W_{III} sample, after its placement on the vertical stage, was aligned so that the beam was slightly above the upper liquid-liquid interface. Samples were scanned at several different vertical positions of the stage. As the

vertical stage position was increased (i.e., as stage moved upward), the vertical position of the bicontinuous phase being exposed to the beam was lowered until passing through the lower liquid-liquid interface. A series of scans across the vertical range of the bicontinuous phase, from top to bottom, is referred to as a "cycle." Most samples were exposed to several consecutive cycles. Operating conditions used for each sample (i.e., τ_{eq}) are given in **Table 1**, including range of vertical distances for the stage, vertical distance interval between scanning positions, number of cycles, and the run time per scan. For example, for τ_{eq} =1 h, each cycle involved collecting scans of *I(Q) vs. Q* data at vertical stage positions of 14, 15, 16, .., 23 mm (i.e., 1 mm length for the vertical distance interval; 10 vertical positions scanned), with 32 consecutive cycles performed. Without accounting for the time required for sample changes, each cycle for τ_{eq} =1 h required 10 x 55 s = 550 s (9.16 min), or collectively for all cycles, 32 x 550 s = 17,600 s (4.9 h). The upper and lower boundaries of the bicontinuous phase were readily determined through the overall scattering intensity, *I(Q)*, and were consistent between all W_{III} samples analyzed for this paper, at vertical stage positions of 14 mm and 23 mm **(Figure S1)**.

SANS data (*I(Q) vs. Q*) were reduced using a standard protocol and analyzed through fitting with a nonlinear general scattering law based on form and structure factors implemented in a Igor Pro software package prepared by personnel at the Center for Neutron Research of the (U.S.) National Institute of Standards, NCNR [36]. *I(Q) vs. Q* data was fit using the TS model [37]:

$$I(Q) = \frac{8\pi\phi(\Delta\rho)^2 \xi^{-1}}{\left(\left(\frac{2\pi}{d}\right)^2 + \xi^{-2}\right)^2 - 2\left(\left(\frac{2\pi}{d}\right)^2 - \xi^{-2}\right)Q^2 + Q^4} + b \qquad (1)$$

where ϕ is the volume fraction of dispersed phase (equivalently water or oil), $\Delta\rho$ the neutron contrast (scattering length density difference), and b is the incoherent background intensity. The parameters ξ and d are the correlation length and quasi-periodic repeat distance, respectively, where the former represents the average length of the interfacial region for which surfactant motion is correlated and is inversely proportional to the interfacial area, while the latter is the average distance across adjacent water plus oil nanodomains. An additional parameter derived from the TS model is the amphiphilicity factor, f_a, which provides a scale of the extent of ordering for the BME water-oil interfaces [37]:

$$f_a = \frac{1-\left(\frac{2\pi\xi}{d}\right)^2}{1+\left(\frac{2\pi\xi}{d}\right)^2} \quad (2)$$

f_a ranges from +1 (completely disordered interface; inability to form a cohesive monolayer) to -1 (highly ordered; lamellar phase) [37]. The wetting-nonwetting transition occurs near f_a = -0.33, above which a bicontinuous phase wets one of the two excess phases and below which the phase form a lens (i.e., a separate phase) [37]. When performing the fitting of Eq. 1 to SANS data, data in the lowest Q range (0.003 Å^{-1}, < Q < 0.0085 Å^{-1}) were not used, to improve the fitting of the model to the main portion of the scattering peak. The parameter $\Delta\rho$ was held constant, and the parameters d, ξ, and b were allowed to vary.

RESULTS AND DISCUSSION

Overall approach

After W_{III} samples of the SDS/pentanol system that were equilibrated at different times (τ_{eq} =10 min, 1 h, 4 h, and 1 d), bicontinuous phases were measured using SANS and analyzed for changes in their structural properties in the vertical direction through applying the TS model. The latter fitted the data well, even for scans collected using short run times, such as 30 s and 55 s (for τ_{eq} =10 min and 1 h, respectively; **Table 1**); however, the uncertainty of the model fit increased with decreasing run time per scan and lower equilibration time **(Figures S2-S5)**. **Figures S6-S9** plot the four TS-derived parameters, *d, ξ, f_a*, and *b*, respectively, versus total (equilibration plus relaxation) time at several vertical stage positions. It is clear from the figures that changes of TS parameters vs. time for a given vertical stage position do not fully align between τ_e values. Therefore, the two events, equilibration and relaxation, are uncoupled. Moreover, the transfer of the sample from a microcentrifuge tube to the 1 mm rectangular quartz cells imposes a relaxation process because of the 4.4-fold decrease of the cross-sectional area, leading to the slow rearrangement of molecules within the bicontinuous phase. A significant level of scatter is also observed vs. vertical stage position and time, particularly for samples employing a short exposure time to the beam (τ_{eq} =10 min, cycles 1-11, and τ_{eq}=4 h; **Table 1**), with *d* showing the most consistent trends with respect to time among the parameters **(Figures S6-S9)**. The scatter of the data for τ_{eq} = 10 min and 1 h likely indicates an insufficient amount of time for data collection for obtaining smooth data. Yet, many trends for TS parameters vs. time are evident, as will be discussed below. No anisotropy was observed for any of the two-dimensional camera images, indicating the absence of lamellae, in contrast to BME samples taken near a glass surface of a microfluidic device in the presence of shear (on a micro-level) [24, 25].

As discussed in our previous study [23], changes in d, ξ, and f_a (the latter of which is related to the ξ/d ratio, per Eq. 2) vs. vertical position are often reflective of the change of the surfactant concentration and activity for the oil-water nanodomain interfaces. An increase of surfactant concentration in bicontinuous phases decreases d, ξ, and f_a. Moreover, an increase of surfactant concentration reduces the average size of nanodomains, hence increasing the bicontinuous phases' oil-water interfacial area, and also producing more strongly ordered surfactant monolayers, hence leading to a decrease of f_a [37]. Equivalently, an increase of surfactant concentration causes the scattering curve to narrow and shift to higher Q, since the width of the scattering curve is inversely proportional to ξ and the maximum Q position for the scattering peak, Q_{max}, is inversely proportional to d. In contrast, a decrease of b likely reflects an increase of the local water/oil ratio since partially (30%) deuterated water produces less background scattering than fully hydrogenated oil: dodecane plus pentanol.

Effect of equilibration time on BME properties

The effects of equilibration and relaxation will be discussed separately. **Figure 1** depicts the effect of τ_{eq} on profiles of TS parameters vs. vertical stage position for the first cycle, thereby minimizing any impact due to relaxation. The parameter d decreased significantly with τ_{eq} for most vertical stage positions, suggesting that the activity or concentration of surfactants adsorbed to the interfaces between nanodomains increased **(Figure 1A)**. Perhaps initially a small amount of water and oil was emulsified, and with time, the emulsified solvents gradually partitioned to the W_{III} excess phases (but not to an extent that the volume fraction of the W_{III} phases changed appreciably on a macroscale) [38], or alternatively, surfactant partitioned from the bulk aqueous phase or the lower liquid-liquid interface to the bicontinuous phase's nanodomain interfaces (noting that SDS is water-soluble). The d vs. vertical stage position profile smoothened with an

increase of τ_{eq}. The latter trend is at least partially attributable to the lower scan time per measurement for the shorter equilibration times: τ_{eq} = 10 min and 1 h **(Table 1)**. In general, *d* increased slightly as the vertical stage position increased (i.e., in the downward direction), but to a decreasing extent as τ_{eq} increased, suggesting that more surfactant was present near the upper portion of the bicontinuous phase. This finding agrees with a recent study of a four-phase microemulsion system formed using a low surfactant concentration (three W_{III} phases plus a lamellar phase residing between the water and bicontinuous phases) [22]. For the cited study, the surfactant concentration was higher for the upper half of the bicontinuous phase, with a decrease observed upon the approach of the upper liquid-liquid interface when traveling upward [22]. However, it should be noted that the proximity to equilibrium conditions may differ between the cited and current studies. Moreover, the decrease of *d* in the upward vertical position was particularly strong for the top half of the bicontinuous phase, between vertical stage position 19 mm and 16 mm for all equilibration times (**Figure 1A**). This trend contradicts the results we obtained previously for the same W_{III} system equilibrated in the same 1 mm pathlength quartz cell for 5.5 d, where *d* decreased as the beam moved downward [23]. However, the conditions are not directly comparable because in the previous study, samples were allowed to equilibrate over a much longer relaxation period.

Exceptions to the trend of increasing *d* with increasing stage vertical position did occur. One exception is the small decrease of *d* observed upon the approach to the lower liquid-liquid interface (from vertical stage position 19 mm to 23 mm) for most τ_{eq} values. In addition, for the minimum τ_{eq} value only, 10 min, *d* was much larger near the top liquid-liquid interface (vertical stage position 15 mm) compared to the other vertical positions **(Figure 1A)**. A similar trend was observed for ξ and the value of f_a is significantly lower at vertical stage position 15 mm for τ_{eq} =

10 min **(Figures 1B and 1C)**. This trend very likely represents the presence of emulsified oil or water droplets that are elongated in shape, suspended in the bicontinuous phase near the top liquid-liquid interface [38]. Similarly, Herrera *et al.* (2022) report that during the formation of the W_{III} bicontinuous phase after the mixing of water and oil in the absence of convective mass transfer, d and ξ were higher and f_a lower at the top portion of the bicontinuous compared to the bottom as oil and water diffused from the excess phases into the bicontinuous phase [2]. These results show that a substantial amount of time must be allowed for equilibration of W_{III} systems, at least 4 h and preferably 1 day, to obtain consistent results, and the neutron beam should contact the BME W_{III} phase near the middle vertical position of the BME phase. This duration is consistent with the estimated time for water to diffuse downward through the bicontinuous phase to the aqueous excess phase. Assuming a 1 cm (0.01 m) height for the bicontinuous phase and using the diffusion coefficient for water as 2.3×10^{-9} m^2 s^{-1}, the approximate time for water to diffuse through the bicontinuous phase will be at least $(0.01\text{ m})^2 / 2.3 \times 10^{-9}$ m^2 s^{-1}, or equivalently ~ 12 h. Using the diffusion coefficient for collective motion of BME nanodomains for the SDS/pentanol system, 1.65×10^{-11} m^2 s^{-1}, [39] determined through dynamic light scattering, the time required for self-diffusion of BMEs is approximately $(0.01\text{ m})^2 / 1.65 \times 10^{-11}$ m^2 s^{-1}, or 70.2 d. This would serve as an estimate of the total time required for equilibration. For applications of W_{III} systems in purification, the partitioning of solutes (e.g., of proteins) between W_{III} phases often occurs initially, indicating the need to better understand the structural gradients occurring at short equilibration times to better control the selectivity of the separation [29].

The current study also produced d, ξ, and f_a values that were slightly higher than our previous study, by 6%, 14%, and 5%, respectively [23]. These differences may reflect differences between preparation methods and equilibration conditions in the two studies, particularly

involving the relaxation time and procedure for the samples once transferred to the quartz cell. The deuteration level in water for the former study was also slightly different: 31.2% previously compared to 30.0% for this study.

Vertical position and τ_{eq} had a much lower effect on ξ than for *d*. There is a slight decrease of ξ with τ_{eq} upon the approach of the lower liquid-liquid interface, particularly for τ_{eq} = 1 mo from vertical stage positions 17 mm to 23 mm and more strongly and consistently from 20 mm to 23 mm **(Figure 1B)**. Values of ξ vs. τ_{eq} are in greater agreement near the upper and lower liquid-liquid interfaces than in the middle of the BME phase, with the exception of vertical stage position 15 mm for τ_{eq} =10 min (as discussed above) and τ_{eq} = 1 h for position 23 mm. Similarly, f_a values did not change greatly with τ_{eq}, except near the upper liquid-liquid interface (vertical stage positions 14-15 mm): the lowest value of f_a for all samples measured in this study occurring at τ_{eq} =10 min (-0.64), and a slight decrease of f_a with τ_{eq} observed between 1 h and 1 d **(Figure 1C).** As discussed above, the former trend is likely attributable to the presence of emulsified oil and water, leading to an exceptionally low value of *d*, hence to a low f_a value, per Eq. 2. f_a increased slightly in the downward vertical direction, suggesting a slight disordering of the nanodomain interfaces in the downward direction. For *b*, there is significant scatter in values at all equilibration times, which makes discernment of trends difficult to achieve. However, for both τ_{eq} = 10 min and 1 d, a decrease of *b* in the downward vertical direction is clearly observed in the middle of the bicontinuous phase, which would represent an increase of water concentration **(Figure 1D)**. This result is consistent with findings observed for BMEs using NMR [3, 22] . For the other equilibration times, *b* is also lower in the middle of the bicontinuous phase as compared to the uppermost and lowermost vertical positions. Of interest is the agreement for *b* between equilibration times near the lower liquid-liquid interface.

Effect of multiple vertical scanning cycles on BME properties

The entire dataset of the effect of repeated scanning cycles on profiles of *d, ξ, f_a,* and *b* vs. vertical stage position and τ_{eq} are given **Figures S6-S9**. To simplify the presentation and smoothen the variability of data for samples undergoing the shortest SANS measurement time (τ_{eq} = 10 min, cycles 1-11 and τ_{eq} =1 h), profiles were binned every 3-5 cycles, as described in the **Figure 2** caption, with resultant profiles presented in **Figures 2-5**. Error bars, representing the difference for values between cycles binned together, were not included in the figures to reduce clutter; but, **Figures 2-5** were replotted in the presence of error bars in **Figures S10-S13**, respectively. It is clear that an increase of cycles increased the consistency and smoothness of the data and affected the values of the TS parameters. However, the observed changes for parameters likely reflect both equilibration and relaxation, especially for the data corresponding to τ_{eq} = 10 min and 1 h, where the most significant changes of the TS parameters vs τ_{eq} were observed during the first cycle **(Figure 1)**. Among the four TS parameters, the most significant changes occurred for *d*. For τ_{eq} =10 min and 1 h, the high value of *d* occurring initially near the upper liquid-liquid interface (vertical stage positions 15 mm and 14 mm, respectively), decreased dramatically with relaxation cycles, from 283 Å to 277 Å for τ_{eq} =10 min, for example **(Figures 2A and B)**. A similar trend was observed for ξ at vertical stage position 15 mm and τ_{eq} =10 min, but occurring to a lesser extent, while f_a underwent a slight increase with relaxation cycles under these conditions **(Figures 3A and 4A)**. These results are consistent with the trends observed in **Figure 1** for when τ_{eq} was increased, suggesting that equilibration is the dominant factor rather than relaxation under these conditions. For τ_{eq} =10 min, according to **Figure S9B,** *b* at vertical stage position 15 mm decreased with cycles from 0-2 h (cycles 1-12), increased between 2 and 3

h (cycles 13-17), and reached a plateau after 3 h (cycle 18), suggesting that water volume fraction at first increased, then decreased until reaching a constant value.

For the latter of the consecutive cycles at τ_{eq} =10 min and 1 h, *d* was smallest near the upper liquid-liquid interface and then increased with vertical stage position (i.e., in downward direction) by 5-7 Å, reaching a plateau at the approach of the middle of the bicontinuous phase, vertical stage positions 18-20 mm **(Figures 2A and B)**. For vertical positions in the middle and bottom of the bicontinuous phase, differences in *d* between relaxation cycles were relatively small, there were no consistent patterns, and the variability of *d* decreased at the approach of the lower liquid-liquid interface. For $\tau_{eq} \geq 4$ h, *d* was impacted by equilibration time to a lesser extent **(Figure 1)**; therefore, the impact of the relaxation process under such conditions is more evident. For the first binned group of τ_{eq} = 4 h, *d* was constant at low values of the vertical stage position (14-15 mm) and then increased abruptly (by 5 Å) at positions 16-17 mm, and slowly increased upon the approach of the lower liquid-liquid interface **(Figure 2C)**. For the second binned group, a similar pattern existed, but with the increase of *d* initiating at position 19 mm, in the middle of the BME phase. For the third binned group, *d* remained nearly constant in the vertical direction, except for a slight increase at the approach of the lower liquid-liquid interface. The change of the *d* vs. vertical stage position profile for the second compared to the first binned group for τ_{eq} = 1 d is consistent in trend to what was described above for τ_{eq} = 4 h **(Figure 2D)**. These changes suggest that relaxation time significantly affected observed structural changes in the vertical direction and that at least several hours are required for equilibration after a W_{III} system is exposed to a change in horizontal area. It is therefore likely that the W_{III} system analyzed in **Figure 1** was not fully at equilibrium since it underwent only 1 relaxation cycle. Changes of all four TS parameters with relaxation cycles for τ_{eq} = 1 d and all given vertical positions were

minor, indicating the increased stability of the W_{III} system with increasing equilibration time **(Figures 2D-5D)**.

For all conditions except at τ_{eq} =10 min (as discussed above), ξ vs. vertical stage position profiles changed only slightly and inconsistently with cycles **(Figure 3)**, similar to that described for ξ vs. τ_{eq} in **Figures 1B and S7**. A few of the observable minor changes will now be discussed. Consistent with the observed trends for **Figure 1B** for the first cycle, ξ decreased with time for vertical stage positions 19 mm and 21 mm, near the lower liquid-liquid interface, particularly at τ_{eq} = 10 min, 4 h (first ~7 cycles) and 1 d (for position 21 mm) **(Figure S7D and E)**. For vertical stage position 21 mm, slightly above the lower liquid-liquid interface, f_a increased significantly with time for τ_{eq} = 4h (lattermost 5 cycles) and 1 d **(Figure S8E)**. For *b*, an increase of cycles did not result in a consistent trend, except that the variability for *b* vs. vertical position was reduced **(Figure 5)**. For τ_{eq} = 4 h and total time of 9.7 h and 14.1 h, the *b* vs. vertical stage position profile was consistently flat, except for an increase and decrease of *b* near the upper and lower liquid-liquid interfaces, respectively, indicating that the water concentration was relatively low and high near the upper and lower interface, respectively.

Change of BME properties vs. vertical position for an isolated W_{III} BME (middle) phase

When comparing TS parameter values between bicontinuous phases isolated from a W_{III} system and remaining within a W_{III} system for τ_{eq} =1 mo, values of ξ and *b* were similar; but, the isolated phase (W_{IV} system) had lower values for *d* and f_a, by 22 Å and 0.03 units, respectively. The results indicate that surfactant concentration or activity in the bicontinuous phases is higher and monolayers are more ordered and rigid for the W_{IV} system **(Figure 6)**. For the W_{IV} system,

the parameter *d* decreased slightly (by ~3 Å) upon the approach of the lower interface and then increased by 14 Å when reaching the interface with the bottom, quartz surface, approaching the value of *d* observed in the W_{III} bicontinuous phase **(Figure 6A)**. f_a also increased at the approach of the lower liquid-liquid interface **(Figure 6C)**. These results suggest that the behavior of the bicontinuous phase is perturbed by the solid-liquid interface. Perhaps surfactant near the interface is adsorbing onto the quartz surface, a finding observed in the literature [40]. Other reports describe that bicontinuous phases, when near a polar surface, undergo an increase in ordering, approaching lamellar structure [24, 25]. Perhaps the slight decrease of *d* between vertical stage positions 6 mm and 26 mm **(Figure 6A)** is consistent with this trend; but, the large increase of *d* near the interface is not. In contrast, *b* is significantly lower near the upper, bicontinuous phase-air free surface **(Figure 6D)**, indicating the presence of higher amounts of water. Also, *b* decreased slightly upon the approach of the lower solid-BME interface, likely representing the selective adsorption of water on the quartz surface.

CONCLUSIONS

For the water/1-dodecane/ SDS/1-pentanol/NaCl W_{III} system, SANS measurements using a precise vertical stage sample environment demonstrated that a structural gradient occurred in the vertical direction for the middle, bicontinuous phase. The gradient was dampened with an increase of equilibration time, particularly when greater than 4 h, suggesting the major source of the structural gradient detected herein is due to the W_{III} system not being at equilibrium. An increase of equilibration time increased the effective activity of surfactants at the interface between oil and water nanodomains, observed by a decrease of the TS parameters *d*, ξ, and f_a with time. The greatest change was observed between 10 min and 4 h; however, a noticeable decrease of *d* occurred between 1 d and 1 mo. For a short, 10 min equilibration time, the values

of d and ξ were high and f_a low near the upper liquid-liquid interface initially and the former two decreased sharply and the latter increased with time to ~5 h, indicative of a lower activity of surfactant at the oil-water nanodomain interfaces initially, perhaps reflecting microscopic amounts of emulsified water and oil that are released to the W_{III} excess phases. After this trend abated, a structural gradient formed: the surfactant activity was higher near the upper liquid-liquid interface, but then decreased in the downward vertical direction until reaching the middle of the bicontinuous phase, upon which the structural gradient in the vertical direction was minor. In addition to equilibration, a relaxation process was observed, associated with the transfer of the W_{III} phase from a microcentrifuge tube to a 1 mm rectangular cell (4.4-fold decrease of surface area), most vividly for the 4 h equilibration time, at which the impact of equilibration time is expected to be low. For relaxation, a decrease of d is observed for the lower and middle portions of the BME phase, indicative of an increase of surface activity and leading to a decreased level of the vertical direction structural gradient. We also observed that the water/oil ratio increased in the downward vertical direction in the middle of the bicontinuous phase and less so near the liquid-liquid interfaces. For a W_{IV} bicontinuous phase isolated from a W_{III} system (of low surfactant concentration), we found major changes for TS parameters near the solid (quartz)-BME phase (increase of d and f_a) that we believe reflect the removal of surfactant due to adsorption to the quartz surface on a microscale.

These results prove that, even though W_{III} samples appear to be at equilibrium macroscopically, small but significant changes in structure may occur. Minimally, at least 4 h is needed for the SDS/pentanol W_{III} system employed herein, that is near optimal salinity. W_{III} systems not at optimal conditions or involving natural oils such as isopropyl myristate and limonene will require even longer equilibration times. The current study complements recent

424 investigations of the W_{III} formation process by providing observations of structural changes
425 occurring after the W_{III} system forms macroscopically [2], of relevance to many applications of
426 BMEs, such as serving as template for nanomaterial synthesis and their use in separations and
427 reactions. The current study also provides information on the storage and transport of BMEs,
428 showing impacts on the transfer of W_{III} systems to vessels possessing a difference in cross-
429 sectional area and to structural changes of bicontinuous phases near solid surfaces at the
430 macroscopic level. Additional research is needed to extend this study to additional W_{III} and W_{IV}
431 bicontinuous systems and solid surface chemistries.

432

433 **ACKNOWLEDGEMENTS**

434 Conceptualization of BME experimental design, SANS data acquisition, and interpretation of
435 results was primarily supported as part of the Breakthrough Electrolytes for Energy Storage
436 (BEES), an Energy Frontier Research Center funded by the U.S. Department of Energy (DOE),
437 Office of Science, Basic Energy Sciences (BES) under Award # DE-SC0019409), and is
438 gratefully acknowledged. SANS measurements were performed using the Bio-SANS instrument
439 of the Center for Structural Molecular Biology (FWP ERKP291), a Structural Biology Resource
440 of the U.S. DOE Office of Biological and Environment Research. This research used resources at
441 the High Flux Isotope Reactor, a U. S. DOE Basic Energy Sciences User Facility operated by the
442 Oak Ridge National Laboratory (ORNL). ORNL is operated by UT-Battelle, LLC under
443 Contract No. DE-AC05-00OR22725 with the U.S.

444

445

AUTHORSHIP STATEMENT

Conceptualization: Hayes, Pingali

Methodology: Hayes, Pingali

Validation: Barth, Hayes, Pingali

Formal analysis: Hayes

Investigation: Barth, Hayes, Pingali

Resources: Hayes, Pingali

Data Curation: Hayes

Writing - Original Draft: Hayes

Writing - Review & Editing: all authors

Visualization: Hayes

Supervision: Hayes, Pingali

Project administration: Hayes, Pingali

Funding acquisition: Hayes, Pingali

CONFLICTS OF INTEREST

There are no conflicts to declare.

464 **Table 1.** Information on the equilibration and relaxation process and vertical positions for SANS
465 analysis of BME phases of W_{III} systems

Equilibration Time (τ_{eq})	Vertical stage distance range, mm	Vertical distance interval between scans, mm	Number of cycles	Run time per scan, s
10 min	15-23	2	21	30; 180 [a]
1 h	14-23	1	32	55
4 h	14-23	1	13	160
1 d	14-23	1	6	150
1 mo	14-23	1	1	744
1 mo (W_{IV}) [b]	4-32	2	1	600

466 [a] first and second times are for cycles 1-11 (0-1.4 h) and 12-21 (1.6-4.9 h), respectively; [b] W_{III}
467 BME phase isolated and placed in a 1 mm pathlength rectangular quartz cell.

468

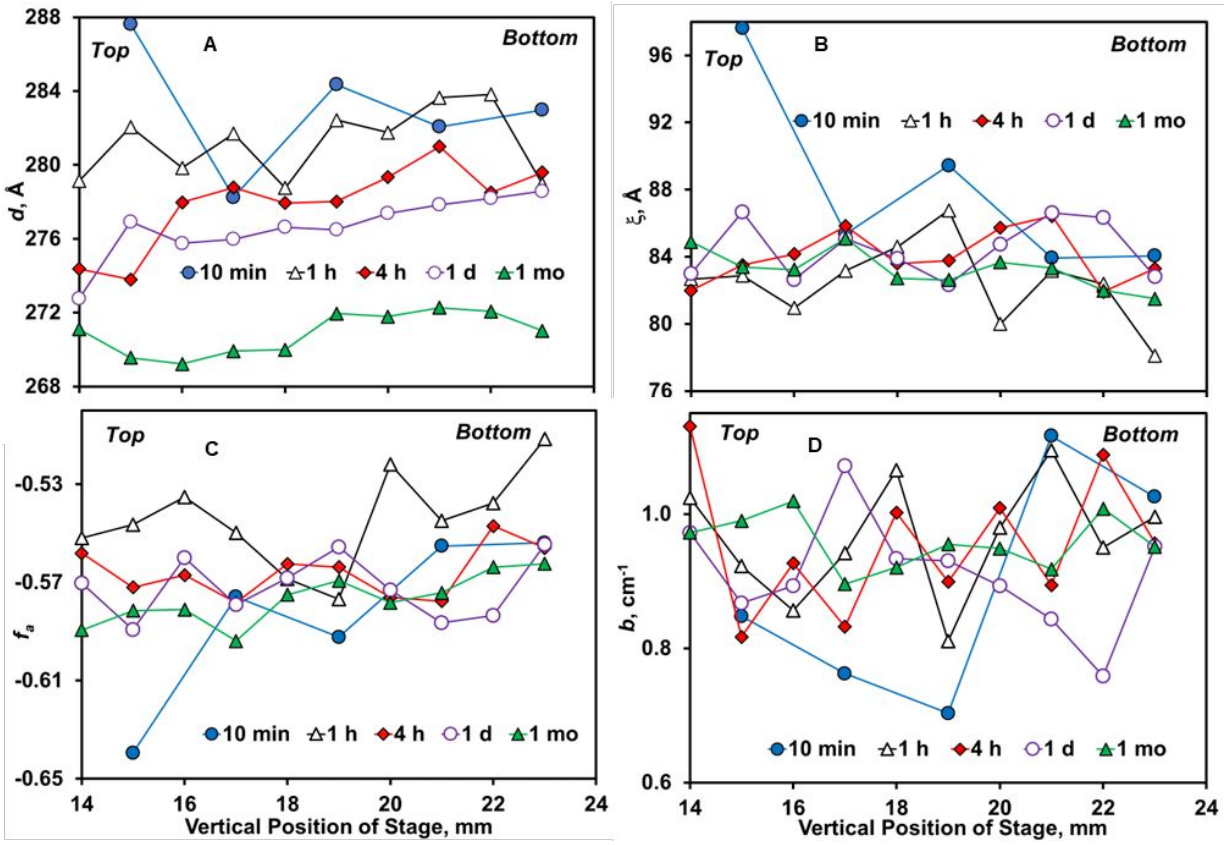

469

470 **Figure 1.** Effect of equilibration time, τ_{eq} (legend) on the change of TS-derived parameters for
471 the middle, bicontinuous phase, of W_{III} systems formed by the Water/SDS/1-pentanol/dodecane
472 system at 22°C vs. vertical stage position. Positions 14 mm and 23 mm are near the top and
473 bottom liquid-liquid interfaces, respectively. **A** quasi-periodic repeat distance (*d*), **B** correlation
474 length (ξ), **C** amphiphilicity factor (f_a), and **D** incoherent background (*b*). Data are from the first
475 analysis cycle. Error bars: *d* (Å) 3.9±0.2, 2.4±0.1, 1.0±0.05,1.1±0.02, 0.4±0.01; ξ (Å) 3.1±0.2,
476 1.9±0.1, 0.9±0.03,1.0±0.01, 0.4±0.01; f_a 0.06±0.004, 0.04±0.002, 0.02±0.001, 0.02±0.001,
477 0.01±0.0002; and *b* (cm^{-1}) 0.01±0.002, 0.01±0.001, 0.003±0.0003, 0.003±0.0003, 0.002±0.0001
478 for τ_{eq} =10 min, 1 h, 4 h, 1 d, and 1 mo, respectively.

479

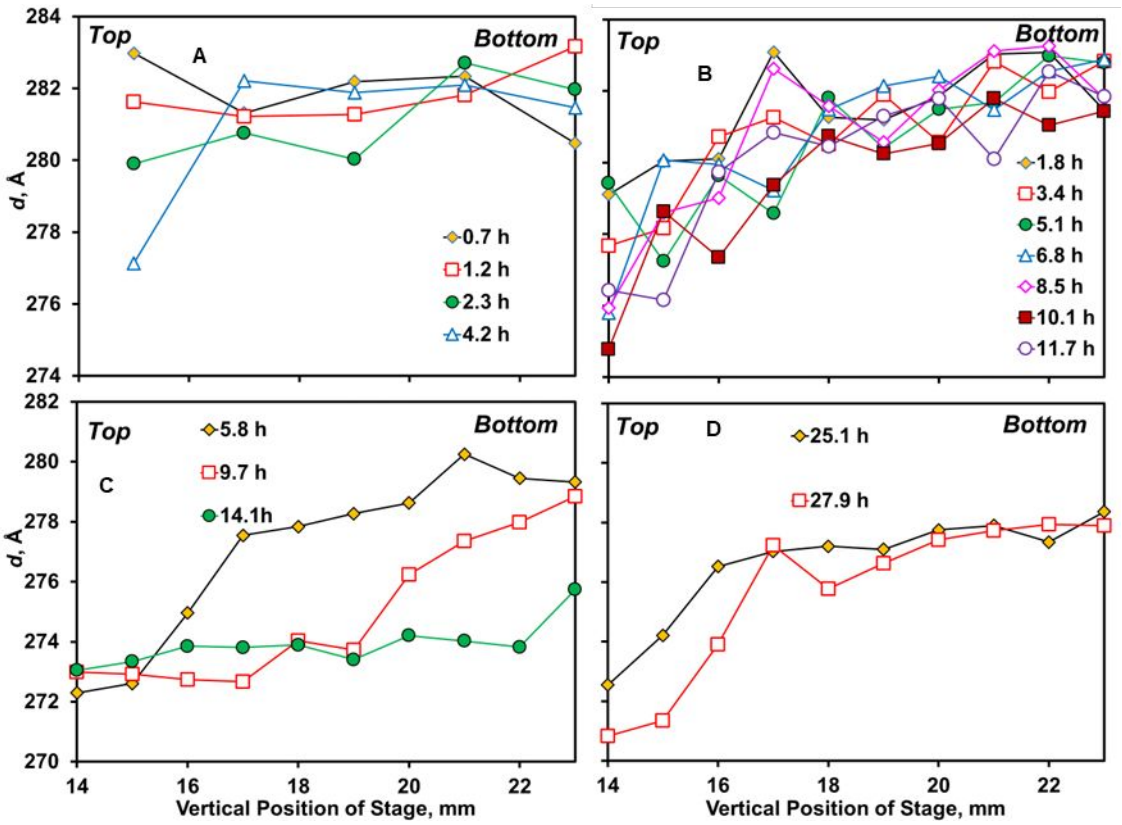

Figure 2. Effect of time for equilibration and relaxation on the change of the quasi-periodic repeat distance, *d*, for the middle, bicontinuous phase, of W_{III} systems formed by the Water/SDS/1-pentanol/dodecane system at 22°C vs. vertical stage position. Positions 14 mm and 23 mm are near the top and bottom liquid-liquid interfaces, respectively. Figs A-D represent equilibration times of 10 min, 1 h, 4 h, and 1 d, respectively, while legends represent total (equilibration + relaxation) time. Each data series represents the average of 5 consecutive relaxation cycles for 10 min and 1 h, 4 cycles for 4 h, and 3 cycles for 1 d. Error bars (standard deviation of the means) for *d* (Å): 2.2±1.2, 2.0±0.7, 1.7±1.0, and 1.2±0.2, for 0.7, 1.2, 2.3, and 4.2 h. respectively (10 min); 1.7±0.5, 1.4±0.7,1.8±0.4, 1.4±0.5, 1.9±0.5, 2.0±0.7, and 2.1±0.8 for 1.8, 3.4, 5.1, 6.8, 8.5, 10.1, and 11.7 h, respectively (1 h), 1.4±0.6, 1.6±0.8, and 0.9±0.3 for 5.8, 9.7, and 14.1 h, respectively (4 h), and 1.1±0.6 and 0.9±0.6 for 25.1 and 27.9h, respectively (1 d).

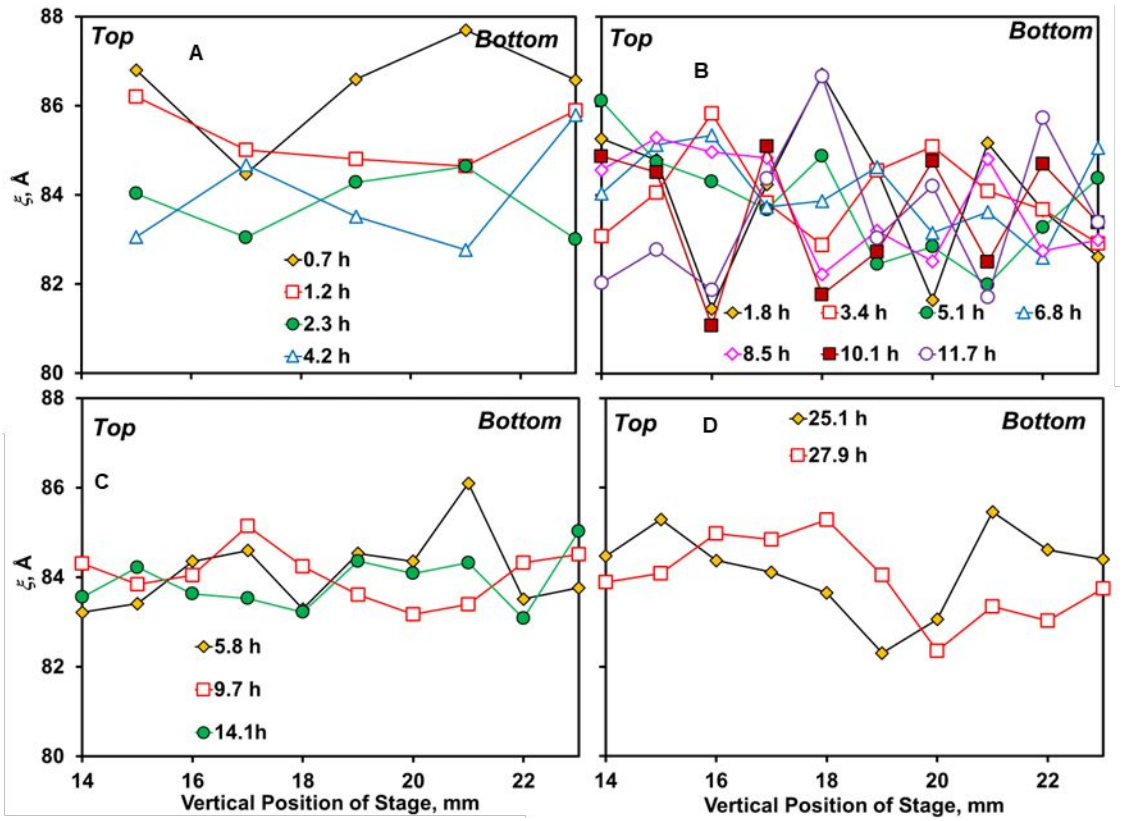

493

494 **Figure 3.** Effect of equilibration and relaxation times on the change of the correlation
495 coefficient, ξ, for the middle, bicontinuous phase, of W_{III} systems formed by the Water/SDS/1-
496 pentanol/dodecane system at 22°C vs. vertical stage position. Positions 14 mm and 23 mm are
497 near the top and bottom liquid-liquid interfaces, respectively. Figs A-D represent equilibration
498 times of 10 min, 1 h, 4 h, and 1 d, respectively, while legends represent total (equilibration +
499 relaxation) time. Each data series represents the average of 5 consecutive relaxation cycles for 10
500 min and 1 h, 4 cycles for 4 h, and 3 cycles for 1 d. Error bars (standard deviation of the means)
501 for ξ (Å): 3.9±1.6, 2.6±0.5, 2.5±0.5, and 1.9±1.0, for 0.7, 1.2, 2.3, and 4.2 h. respectively (10
502 min); 2.2±0.8, 2.5±0.8, 2.6±1.0, 2.4±0.7, 2.6±0.7, 2.5±0.7, and 2.5±0.7 for 1.8, 3.4, 5.1, 6.8, 8.5,
503 10.1, and 11.7 h, respectively (1 h), 1.2±0.4, 1.5±0.7, and 1.5±0.6 for 5.8, 9.7, and 14.1 h,
504 respectively (4 h), and 1.6±0.4 and 1.0±0.6 for 25.1 and 27.9 h, respectively (1 d).

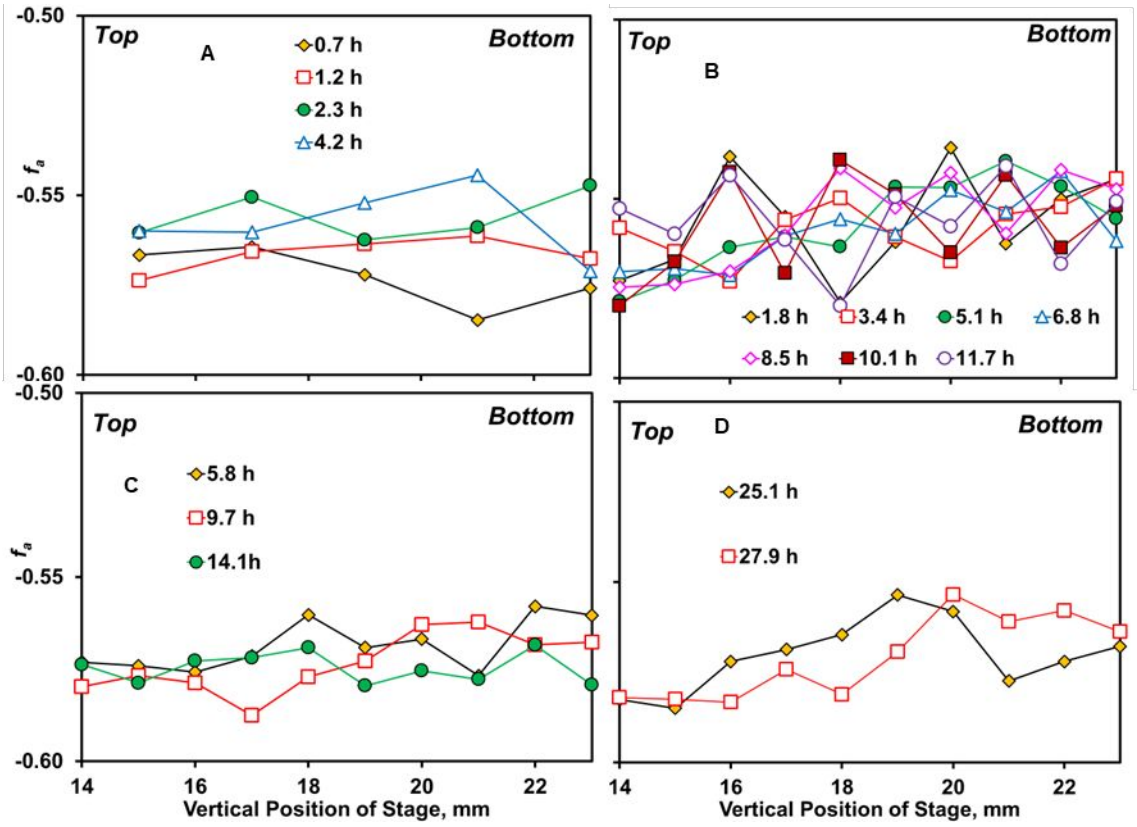

Figure 4. Effect of equilibration and relaxation times on the change of the amphiphilicity factor, f_a, for the middle, bicontinuous phase, of W_{III} systems formed by the Water/SDS/1-pentanol/dodecane system at 22°C vs. vertical stage position. Positions 14 mm and 23 mm are near the top and bottom liquid-liquid interfaces, respectively. Figs A-D represent equilibration times of 10 min, 1 h, 4 h, and 1 d, respectively, while legends represent total (equilibration + relaxation) time. Each data series represents the average of 5 consecutive relaxation cycles for 10 min and 1 h, 4 cycles for 4 h, and 3 cycles for 1 d. Error bars (standard deviation of the means) for f_a: 0.028±0.011, 0.018±0.004, 0.020±0.003, and 0.016±0.008 for 0.7, 1.2, 2.3, and 4.2 h. respectively (10 min); 0.017±0.006, 0.021±0.008, 0.021±0.009, 0.018±0.006, 0.020±0.005, 0.019±0.006, and 0.019±0.004 for 1.8, 3.4, 5.1, 6.8, 8.5, 10.1, and 11.7 h, respectively (1 h), 0.009±0.003, 0.011±0.004, and 0.011±0.005 for 5.8, 9.7, and 14.1 h, respectively (4 h), and 0.013±0.004 and 0.007±0.005 for 25.1 and 27.9 h, respectively (1 d).

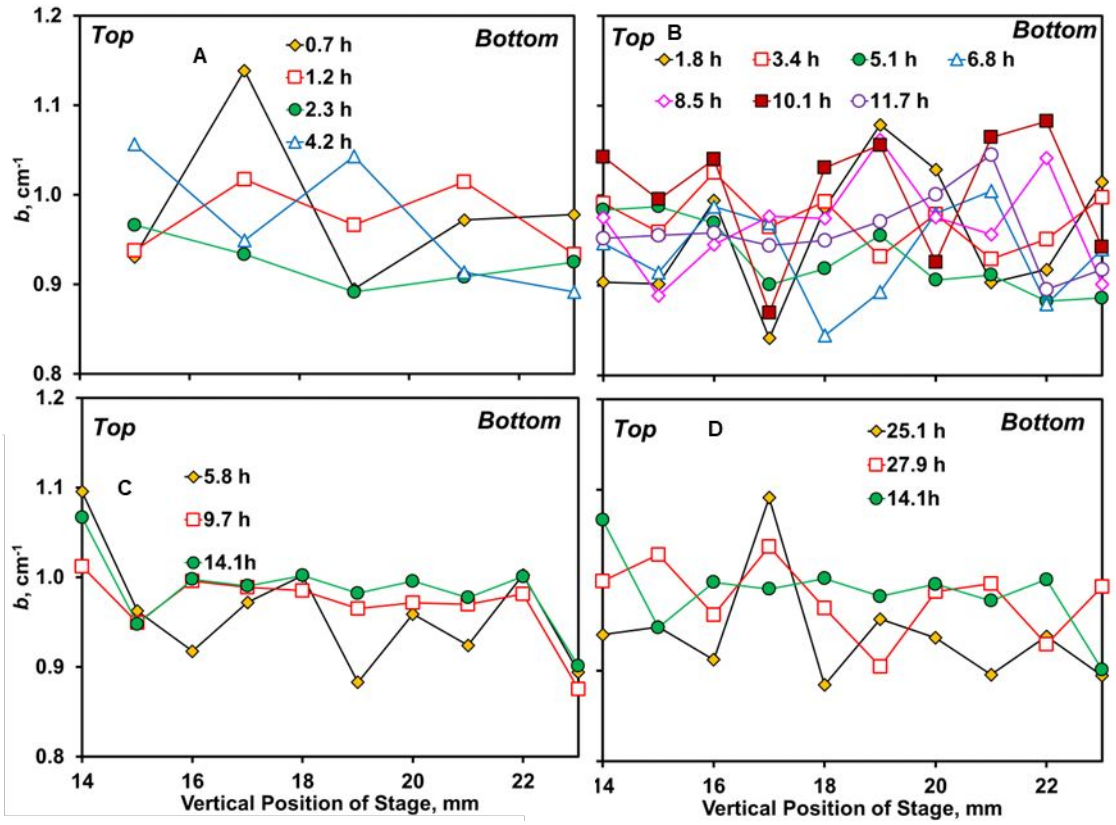

Figure 5. Effect of equilibration and relaxation times on the change of the background, *b*, for the middle, bicontinuous phase, of W_{III} systems formed by the Water/SDS/1-pentanol/dodecane system at 22°C vs. vertical stage position. Positions 14 mm and 23 mm are near the top and bottom liquid-liquid interfaces, respectively. Figs A-D represent equilibration times of 10 min, 1 h, 4 h, and 1 d, respectively, while legends represent total (equilibration + relaxation) time. Each data series represents the average of 5 consecutive relaxation cycles for 10 min and 1 h, 4 cycles for 4 h, and 3 cycles for 1 d. Error bars (standard deviation of the means) for *b* (cm^{-1}): 0.210±0.049, 0.176±0.060, 0.083±0.025, and 0.075±0.022 for 0.7, 1.2, 2.3, and 4.2 h. respectively (10 min); 0.131±0.070, 0.148±0.054, 0.097±0.024, 0.124±0.056, 0.136±0.032, 0.118±0.064, and 0.146±0.054 for 1.8, 3.4, 5.1, 6.8, 8.5, 10.1, and 11.7 h, respectively (1 h), 0.069±0.048, 0.067±0.027, and 0.081±0.038 for 5.8, 9.7, and 14.1 h, respectively (4 h), and 0.077±0.045 and 0.081±0.052 for 25.1 and 27.9 h, respectively (1 d).

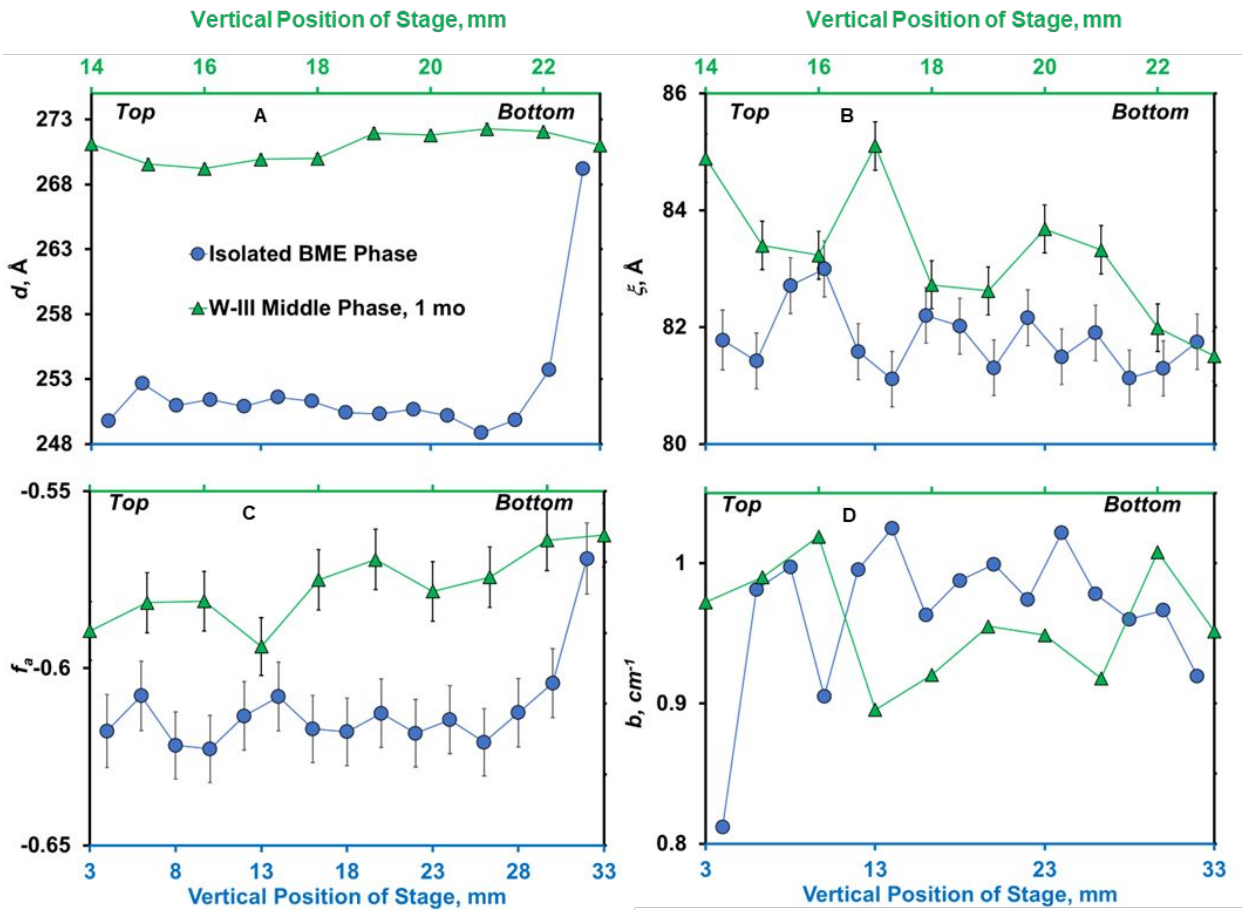

Figure 6. Effect of vertical stage position vs. parameter values derived from the Teubner-Strey model applied to SANS data for a W_{III} system formed by the Water/SDS/1-pentanol/dodecane system at 22°C, equilibrated for 1 mo. Comparison between a bicontinuous phase within a W_{III} system and a bicontinuus phase isolated from the W_{III} system and placed in a quartz rectangular cuvette. **A** quasi-periodic repeat distance (*d*), **B** correlation length (ξ), **C** amphiphilicity factor (f_a), and **D** incoherent background (*b*).

REFERENCES

1. J.-L. Salager, A. M. Forgiarini, R. E. Antón and L. Quintero, *Energy Fuels*, 2012, **26**, 4078-4085.
2. D. Herrera, T. Chevalier, D. Frot, L. Barré, A. Drelich, I. Pezron and C. Dalmazzone, *Journal of Colloid and Interface Science*, 2022, **609**, 200-211.
3. M. I. Velasco, A. Iborra, J. M. Giussi, O. Azzaroni and R. H. Acosta, *Langmuir*, 2022, **38**, 15226-15233.
4. X. Li and X. Huang, *Colloids and Surfaces A: Physicochemical and Engineering Aspects*, 2022, **655**, 130254.
5. A. E. Imel, B. Barth, D. G. Hayes, M. Dadmun and T. Zawodzinski, *ACS Applied Materials & Interfaces*, 2022, **14**, 20179-20189.
6. K. Nakao, K. Noda, H. Hashimoto, M. Nakagawa, T. Nishimi, A. Ohira, Y. Sato, D. Kato, T. Kamata, O. Niwa and M. Kunitake, *Journal of Colloid and Interface Science*, 2023, **641**, 348-358.
7. Y. Zheng, Á. P. Ramos, H. Wang, G. Álvarez, A. Ridruejo and J. Peng, *Materials Today Energy*, 2023, **34**, 101286.
8. E. T. Adesuji, V. O. Torres-Guerrero, J. A. Arizpe-Zapata, M. Videa, M. Sánchez-Domínguez and K. M. Fuentes, *Nanotechnology*, 2020, **31**, 425601.
9. M. Abutalip, G. Zhigerbayeva, D. Kanzhigitova, P. Askar, Y. Yeszhan, T. T. Pham, S. Adilov, R. Luque and N. Nuraje, *Advanced Materials*, 2023, **35**, 2208864.
10. R. Arabjamaloei, R. S. Shah, S. Bryant and M. Trifkovic, *Physics of Fluids*, 2021, **33**.

11. W.-J. Cho, S.-K. Cho, J. H. Lee, J. H. Yoon, S. Kwon, C. Park, W. B. Lee, P. J. Yoo, M. Lee, S. Park, T. H. Kang and G.-R. Yi, *Journal of Materials Chemistry A*, 2023, **11**, 1676-1683.
12. S. Shiba, S. Yoshimoto, S. Hashiguchi, M. Kunitake, D. Kato, O. Niwa and M. Matsuguchi, *Electrochimica Acta*, 2022, **426**, 140761.
13. K.-O. Choi, S. J. Choi and S. Lee, *Food Chemistry*, 2021, **359**, 129875.
14. K. Peng, T. Sottmann and C. Stubenrauch, *Molecular Physics*, 2021, **119**, e1886363.
15. M. A. Oehler, D. G. Hayes, D. H. D'Souza, M. Senanayake, V. Gurumoorthy, S. V. Pingali, H. M. O'Neill, W. Bras and V. S. Urban, *Journal of Surfactants and Detergents*, 2023, **26**, 387-399.
16. M. B. Sims, J. W. Goetze, G. D. Gorbea, Z. M. Gdowski, T. P. Lodge and F. S. Bates, *ACS Applied Materials & Interfaces*, 2023, **15**, 10044-10052.
17. B. Zhang, S. Cui, T. P. Lodge and F. S. Bates, *Macromolecules*, 2023, **56**, 1663-1673.
18. T. T. L. Nguyen, A. Edelen, B. Neighbors and D. A. Sabatini, *Journal of Colloid and Interface Science*, 2010, **348**, 498-504.
19. J. C. Lopez-Montilla, S. Pandey, D. O. Shah and O. D. Crisalle, *Water Res.*, 2005, **39**, 1907-1913.
20. D. G. Hayes, R. Ye, R. N. Dunlap, M. J. Cuneo, S. V. Pingali, H. M. O'Neill and V. S. Urban, *Colloids and Surfaces B: Biointerfaces*, 2017, **160**, 144-153.
21. J. Sjoblom, R. Lindberg and S. E. Friberg, *Advances in Colloid and Interface Science*, 1996, **65**, 125-287.
22. K. Ishikawa, M. Behrens, S. Eriksson, D. Topgaard, U. Olsson and H. Wennerström, *The Journal of Physical Chemistry B*, 2016, **120**, 6074-6079.

23. D. G. Hayes, S. V. Pingali, H. M. O'Neill, V. S. Urban and R. Ye, *Soft Matter*, 2018, **14**, 5270-5276.

24. J. Fischer, L. Porcar, J. T. Cabral and T. Sottmann, *Soft Matter*, 2023, DOI: 10.1039/D3SM00558E.

25. J. Fischer, L. Porcar, J. T. Cabral and T. Sottmann, *Journal of Colloid and Interface Science*, 2023, **635**, 588-597.

26. F. Lipfert, O. Holderer, H. Frielinghaus, M.-S. Appavou, C. Do, M. Ohl and D. Richter, *Nanoscale*, 2015, **7**, 2578-2586.

27. M. Kerscher, F. Lipfert and H. Frielinghaus, *Chemistry Africa*, 2020, **3**, 703-709.

28. M. Gvaramia, G. Mangiapia, P. Falus, M. Ohl, O. Holderer and H. Frielinghaus, *Journal of Colloid and Interface Science*, 2018, **525**, 161-165.

29. J. A. Gomez del Rio and D. G. Hayes, *Biotechnology Progress*, 2011, **27**, 1091-1100.

30. D. G. Hayes, R. Ye, R. N. Dunlap, D. B. Anunciado, S. V. Pingali, H. M. O'Neill and V. S. Urban, *Biochimica et Biophysica Acta (BBA) - Biomembranes*, 2018, **1860**, 624-632.

31. A. M. Bellocq and D. Gazeau, *Prog. Colloid Polym. Sci*, 1988, **76**, 203-210.

32. J. A. Silas and E. W. Kaler, *Journal of Colloid and Interface Science*, 2003, **257**, 291-298.

33. D. G. Hayes, J. A. Gomez del Rio, R. Ye, V. S. Urban, S. V. Pingali and H. M. O'Neill, *Langmuir*, 2015, **31**, 1901-1910.

34. V. K. Sharma, D. G. Hayes, V. S. Urban, H. M. O'Neill, M. Tyagi and E. Mamatov, *Soft Matter*, 2017, **13**, 4871-4880.

35. W. T. Heller, V. S. Urban, G. W. Lynn, K. L. Weiss, H. M. O'Neill, S. V. Pingali, S. Qian, K. C. Littrell, Y. B. Melnichenko, M. V. Buchanan, D. L. Selby, G. D. Wignall, P. D. Butler and D. A. Myles, *J. Appl. Crystallogr.*, 2014, **47**, 1238-1246.

36. S. R. Kline, *J. Appl. Crystallogr*, 2006, **39**, 895-900.

37. K. V. Schubert, R. Strey, S. R. Kline and E. W. Kaler, *J. Chem. Phys.*, 1994, **101**, 5343-5355.

38. J.-L. Salager, R. Marquez, M. Rondón, J. Bullón and A. Graciaa, *ACS Omega*, 2023, **8**, 9040-9057.

39. V. K. Sharma, D. G. Hayes, V. S. Urban, H. O'Neill, M. Tyagi and E. Mamontov, *Journal of Colloid and Interface Science*, 2021, **590**, 94-102.

40. X. Zhou, J.-T. Liang, C. D. Andersen, J. Cai and Y.-Y. Lin, *Colloids and Surfaces A: Physicochemical and Engineering Aspects*, 2018, **553**, 397-405.